

Electronic supplementary information:

Leakage-free polypyrrole-Au nanostructures for combined Raman detection and photothermal cancer therapy

Xiaojun Luo, Xiaoyan Liu, Yinuo Pei, Yawen Ling, Ping Wu,* and Chenxin Cai*

Jiangsu Key Laboratory of New Power Batteries, Jiangsu Collaborative Innovation Center of Biomedical Functional Materials, National and Local Joint Engineering Research Center of Biomedical Functional Materials, College of Chemistry and Materials Science, Nanjing Normal University, Nanjing 210097, P.R. China.

* Corresponding author, E-mail: wuping@njnu.edu.cn (P. Wu); cxcai@njnu.edu.cn (C. Cai)

1. Biocompatibility of the S2.2-PPy-Au nanostructures. MTT (3-(4,5-dimethylthiazol-2-yl)-2,5-diphenyltetrazolium bromide) measurements were performed to evaluate the biocompatibility of the S2.2-Ppy-Au nanostructures. For MTT measurements, MCF-7 cells ($\sim 1 \times 10^4$) were first incubated with S2.2-Ppy-Au nanostructures at a concentration of 0–200 $\mu\text{g mL}^{-1}$ for 12 h, and were repeatedly rinsed with PBS to remove the nonspecifically bound nanocomposites. 10 μL of MTT solution (5 mg mL^{-1} in PBS, pH 7.4) was then added into each well and incubated for 4 h at 37 °C. Afterwards, 100 μL of dimethylsulfoxide (DMSO) was added into each well. Absorbance was recorded at 550 nm on a Synergy 2 microplate reader (Biotek, USA). The viabilities of the cells incubated with the S2.2-Ppy-Au nanostructures were obtained by comparing with those of the cells without incubation of the nanostructures (their viability was taken as 100% as a control).

2. LDH Assay. MCF-7 cells were placed in 96-well plates ($\sim 1 \times 10^4$ cells each well) and incubated for 24h. Then, S2.2-PPy-Au nanostructures (100 $\mu\text{g mL}^{-1}$, 1 mL) were introduced to each well. After 2 h incubation, the cells were irradiated under an 808 nm laser at a power density of 0.5 W cm^{-2} for 20 min, and the plates were then equilibrated at room temperature for 30 min. CytoTox-ONE reagent (100 μL , Sigma) was added to each well, and the plates were incubated for 10 min at room temperature. The fluorescence signal at 590 nm was recorded with an excitation source of 560 nm on a Synergy 2 microplate reader. LDH release was expressed relative to the basal LDH release from untreated cells.

3. Caspase-3 Activity Assay. The cells were seeded into 96-well plates ($\sim 1 \times 10^4$ cells/well) and allowed to attach for 24 h. After incubation with the S2.2-PPy-Au nanostructures (100 $\mu\text{g mL}^{-1}$, 1 mL) for 2 h and irradiation at 0.5 W cm^{-2} for 20 min, Caspase-Glo3/7 reagent (100 μL , Promega) was added to each well, followed by incubation at room temperature for 30 min. The caspase 3/7 activity was evaluated by recording the luminescence of each sample using a microplate reader.

4. Figures.

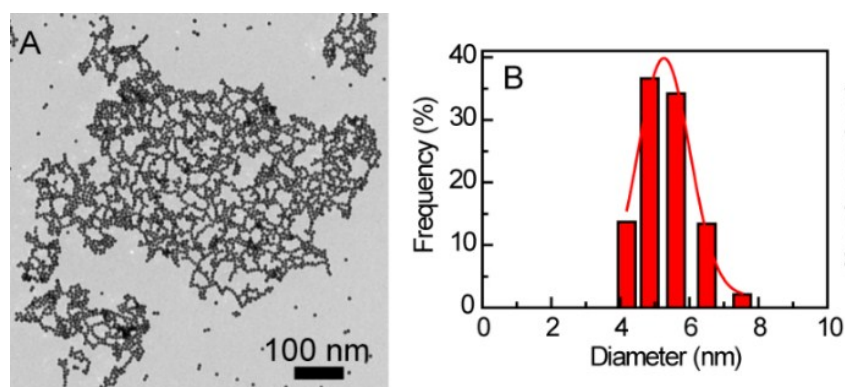


Fig. S1. (A) Typical TEM image of the prepared Au NPs. (B) Size distribution of the prepared Au NPs.

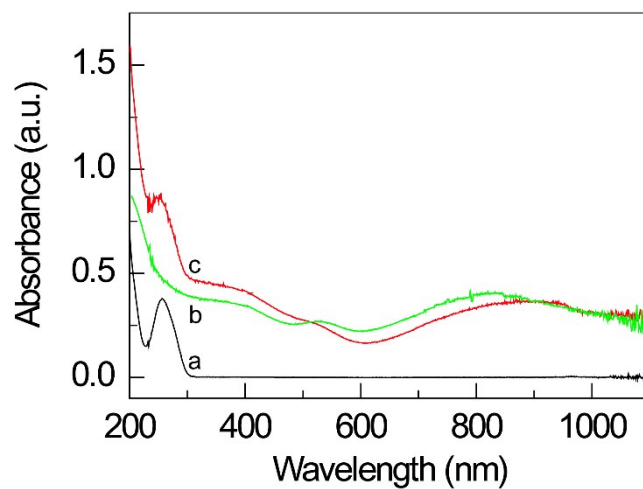


Fig. S2. UV-Vis-NIR spectra of aptamer S2.2 solution (a), PPy-Au nanostructures (b), and S2.2-PPy-Au nanostructures (c) suspension.

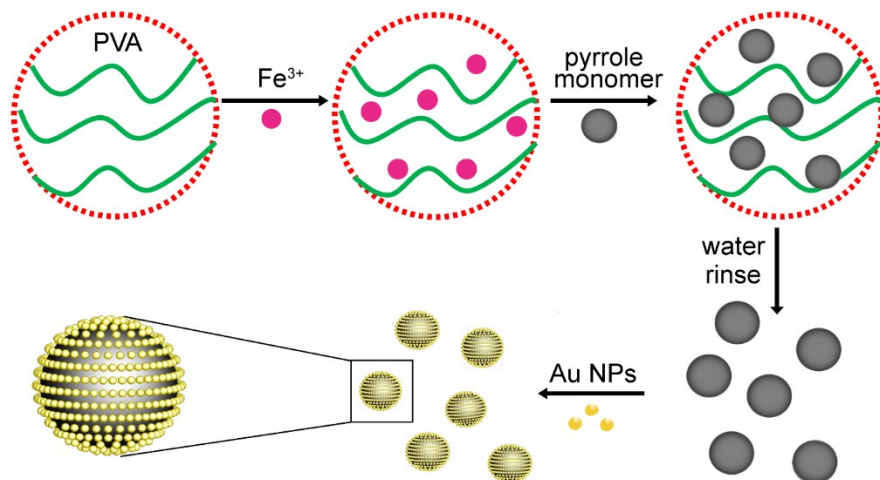


Fig. S3. Schematic illustration of synthesis process of PPy-Au nanostructures.

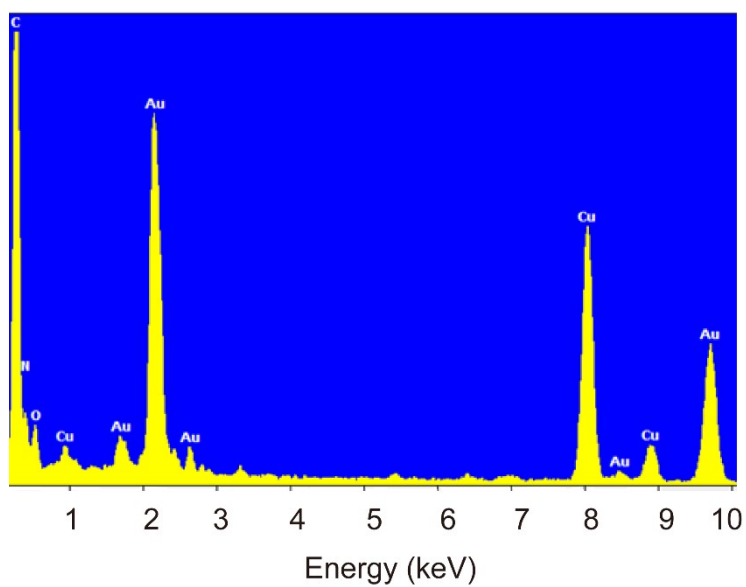


Fig. S4. EDX spectrum of the synthesized PPy-Au nanostructures.

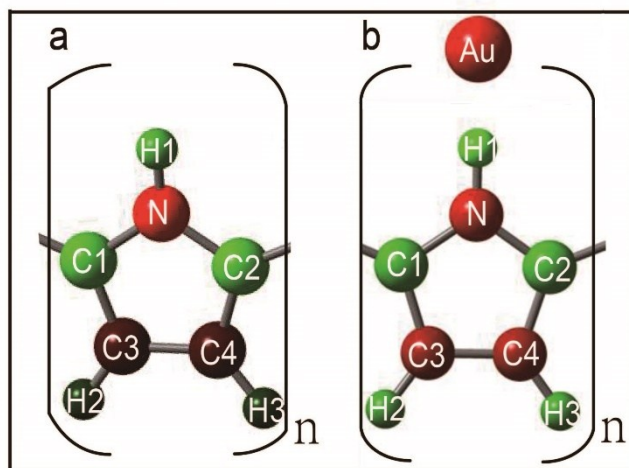


Fig. S5. Calculated charge distribution on each atom in one of pentagon ring in PPy without (a) and with Au atom.

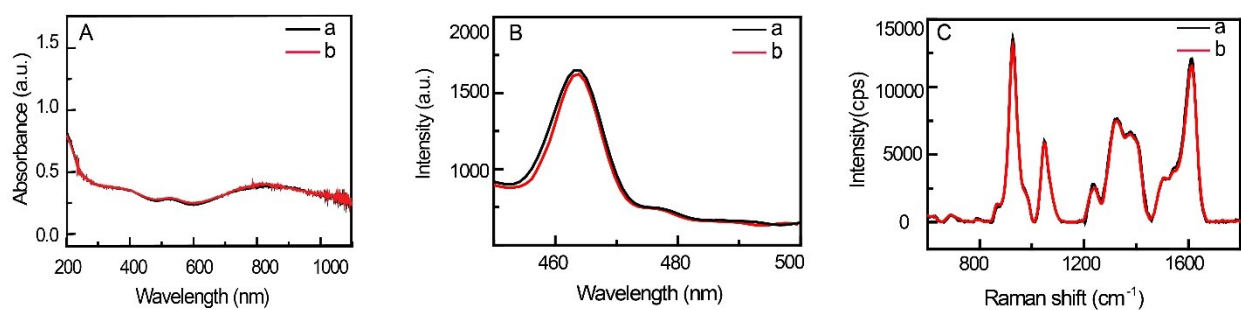


Fig. S6 (A) UV-vis-NIR, (B) photoluminescent, and (C) Raman spectra of fresh synthesized PPy-Au nanostructures (a) and PPy-Au nanostructures after four weeks preparation.

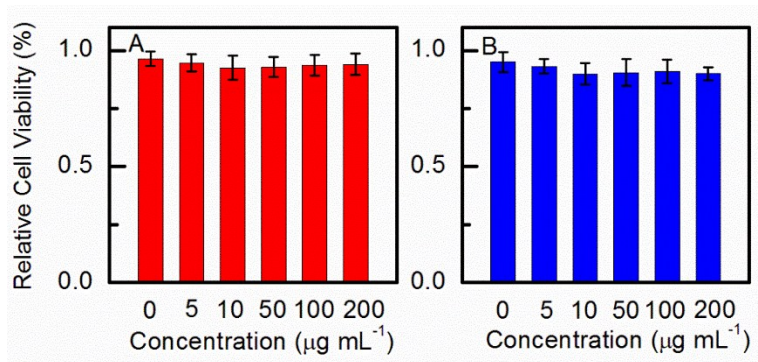


Fig. S7. MTT assay for MCF-7 cells upon incubation of S2.2-PPy-Au nanostructures of concentrations ranging from 0 to 200 $\mu\text{g mL}^{-1}$.

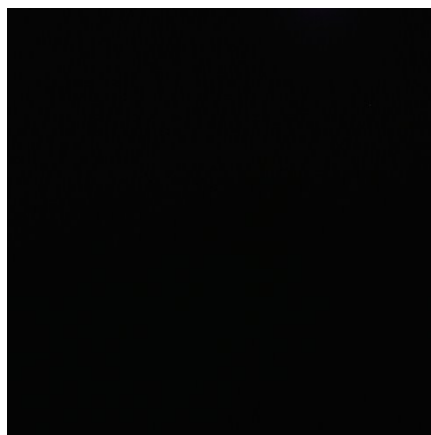


Fig. S8. Fluorescence image of MCF-7 cells without incubation with S2.2-PPy-Au nanostructures. The fluorescence image was captured under excitation at 405 nm.

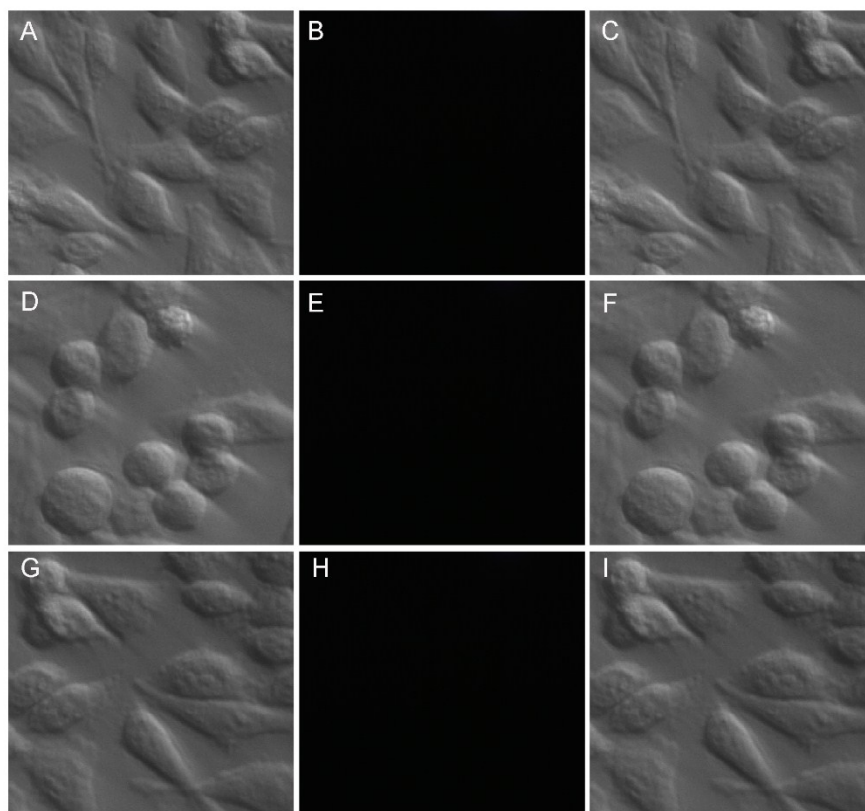


Fig. S9. (A, D, G) DIC, (B, E, H) Fluorescence, and (C, F, I) overlapped images of HepG2 (upper panel) MDA-MB-453 (middle panel), and MCF-10A (under panel) cells after incubation with S2.2-PPy-Au nanostructures. The fluorescence images were captured under excitation at 405 nm.

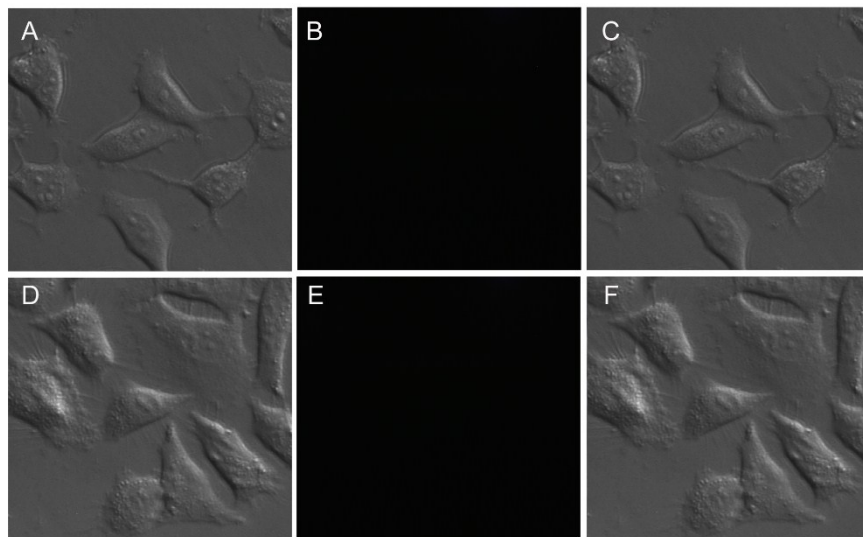


Fig. S10. (A, D) DIC, (B, E) Fluorescence, and (C, F) overlapped images of MCF-7 cells after incubation with DNA (having three mismatched bases in comparison with S2.2)-PPy-Au nanostructures (upper panel) and Sgc8-PPy-Au nanostructures (under panel). The fluorescence images were captured under excitation at 405 nm.

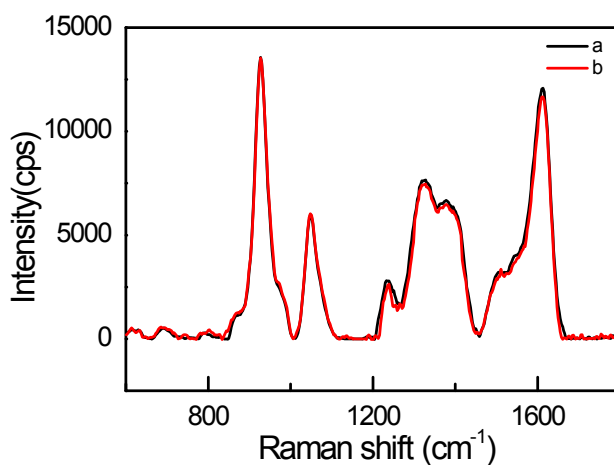


Fig. S11 Raman spectra of S2.2-PPy-Au nanostructures dispersed in PBS (curve a, pH 7.4) and PBS (curve b, pH 5.5).

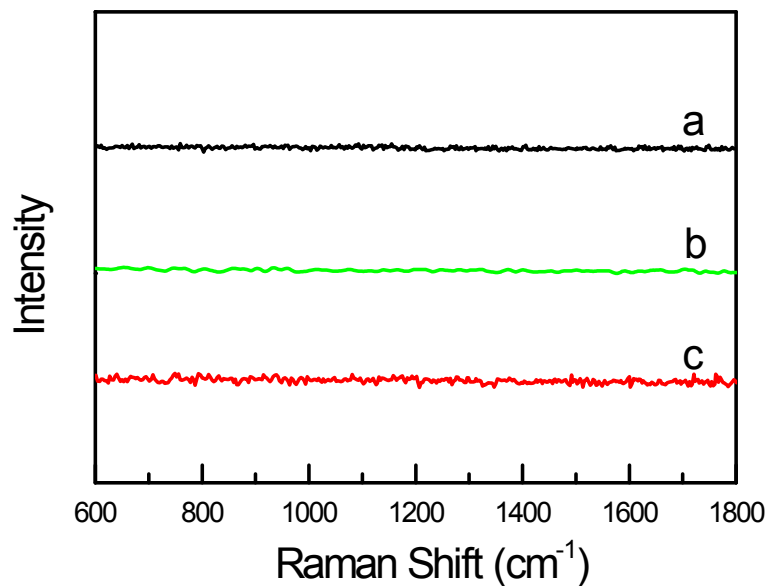


Fig. S12 Raman spectra of the HepG2 (a), MDA-MB-453 (b), and MCF-10A (c) cells after incubation with the S2.2-PPy-Au nanostructures.

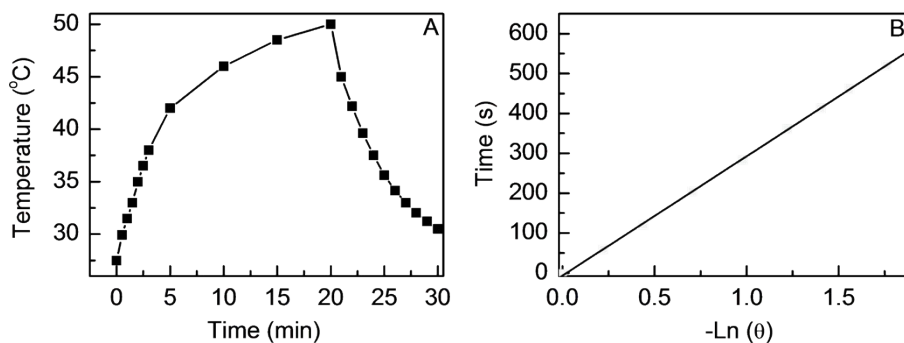


Fig. S13 (A) The course of the temperature of the PPy NSs ($100 \mu\text{g mL}^{-1}$) and Au NPs ($100 \mu\text{g mL}^{-1}$) mixture under 808 nm laser irradiation at a power density of 0.5 W cm^{-2} for 20 min, followed by cooling

to room temperature after turning off the laser. (B) Plot of the cooling time as a function of the negative natural logarithm of the temperature driving force obtained from the cooling stage, as shown in (A).

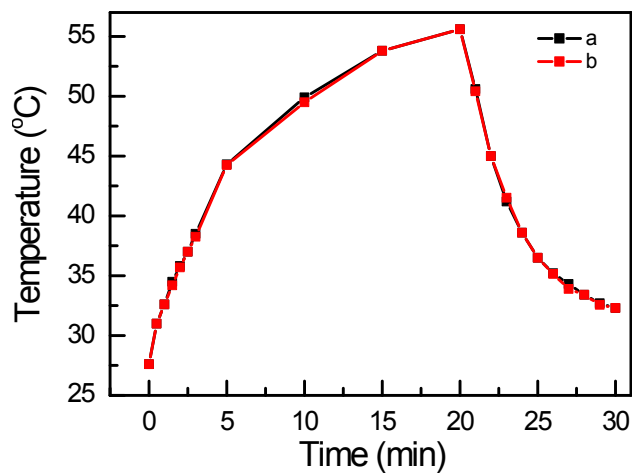


Fig. S14 Temperature profiles as a function of the irradiation time for the $100 \mu\text{g mL}^{-1}$ PPy-Au nanostructures dispersed in PBS (a, pH 7.4) and PBS (b, pH 5.5) under irradiation from an 808 nm laser at a power density of 0.5 W cm^{-2} .

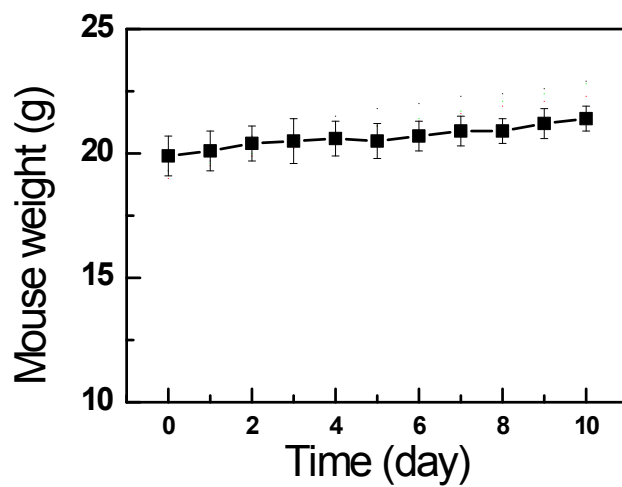


Fig. S15. The body weight of mice in group I after PTT.

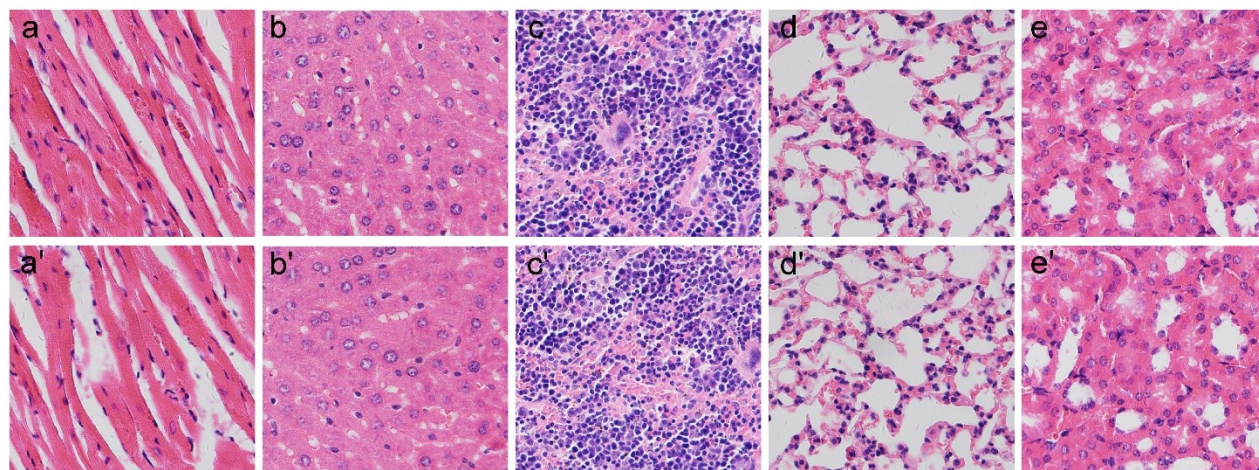


Fig. S16. Typical pathological slices of the heart, liver, spleen, lung, and kidney from mice injected with S2.2-PPy-Au nanostructures (a-e) and irradiated and control group (without any treatment) (a'-e').